JOURNAL OF MATERIALS SCIENCE 19 (1984) 3796–3805

A double-torsion study of the fracture of polyethersulphone

P. J. HINE, R. A. DUCKETT, I. M. WARD
Department of Physics, University of Leeds, Leeds, UK

Fracture studies of polyethersulphone have been undertaken using the double torsion geometry, in particular to establish the effects of ageing and crack speed on fracture toughness. The stability of crack growth was found in all cases to be very dependent on initial notching. If by suitable techniques, e.g. fatigue, a craze was formed at the notch root the subsequent crack growth was found to be stable, with a craze ahead of the growing crack. Under these conditions only a slight dependence of fracture toughness on crack speed was observed, with no significant differences between material aged for 5 years at room temperature and freshly moulded samples. The dimensions of the observed craze were found to be very similar to those of crazes observed in a parallel study using compact tension geometry and lead to comparable values for craze stress and crack opening displacement. In many instances unstable crack growth was observed, often described as "stick–slip". This was often associated with the absence of a craze at the crack tip, perhaps due to a damage zone created during razor notching. The initiation load and load for crack arrest were determined and used to calculate initiation and arrest values for the fracture toughness as a function of the applied deformation rate. It was found that these values converged at high crosshead speeds to a value independent of ageing, although for the freshly moulded material the initiation values were significantly higher, and the arrest values lower. Electrically conducting grids were used to establish that crack speeds up to 400 m sec^{-1} occur during stick–slip crack growth. A detailed discussion is presented of conditions required for stable and unstable crack growth in polyethersulphone.

1. Introduction

The work presented in this paper forms part of a comprehensive investigation of the fracture behaviour of polyethersulphone. In a recent paper we described a combination of fracture toughness measurements using compact tension specimens with an optical examination of the craze and shear lips at the tip of the crack [1]. In the present paper a complementary study using the double torsion test is presented. The double torsion test has been extensively used to study the fracture behaviour of brittle polymers, especially epoxy resins [2–7] and modified epoxy resins [8–10] and polymethylmethacrylate [11, 12]. In the studies described here, the fracture behaviour has been examined as a function of crack speed, on samples of polyethersulphone which have been either freshly prepared or aged. As in our previous studies [1], the optical interference pattern at the crack tip has been examined with a view to comparing the craze shape with that predicted by the Dugdale zone model so that parameters such as the crack opening displacement and craze stress can be determined [13–16].

2. Experimental details

2.1. Materials

The fracture toughness tests were undertaken on two types of material, plaques which had been freshly prepared for the present investigation (material I), and plaques moulded five years previously and aged under ambient conditions (material II).

0022–2461/84 $03.00 + .12

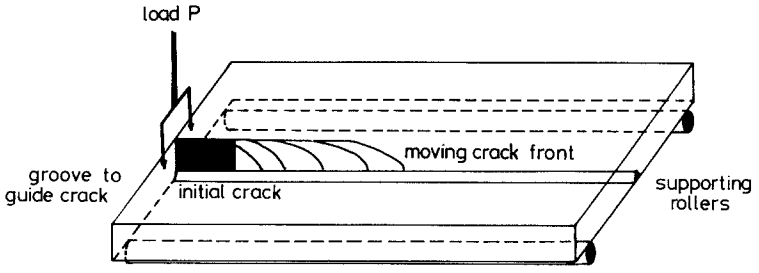

Figure 1 Double torsion specimen.

2.2. Measurements of modulus and yield stress

The modulus of each type of sample was determined in four-point bend loading. The yield stresses were obtained from load–extension curves determined in tension on dumb-bell specimens. Both these tests were performed in an Instron tensile testing machine.

2.3. The double torsion test

The double torsion test was first investigated by Evans [17] with particular reference to determining the variation in fracture toughness, K_c, with crack speed. In this respect the test has the advantage that the crack propagates at a constant value of the stress intensity factor.

The double torsion test which we have used is based on the procedures of Kies and Clark [18], following a method devised by Outwater. The specimen is of rectangular form with a notch at one end and a central V groove running along its lower face. The specimen is supported on two parallel rollers and loaded through two hemispheres positioned over the notch (Fig. 1). During loading the crack is guided by the centre groove as it propagates across the sample.

Two sizes of double torsion rig were constructed, one with a moment arm of 7.5 mm and the other with a moment arm of 25 mm, using samples of width 26.5 and 76.5 mm, respectively. The large rig was the maximum size possible for the size of plaques available (76.5 mm x 100 mm injection moulded by the Ministry of Defence from polymer supplied by ICI Ltd), whereas the smaller rig gave a better length to width ratio.

A groove was needed to guide the crack along the centre of the sample during propagation. This was introduced with a shaping maching, and an angle of 60° was used. To encourage the crack to travel along this path a razor blade was run along the bottom of the groove before loading commenced. Care was always taken to ensure that the sample was positioned centrally and parallel with respect to the supporting rollers.

Another important consideration was the production of the initial starting notch. In the first tests performed the notching was accomplished by pushing a razor blade into an initial saw cut along the centre groove. Other methods were tried, and these will be discussed in a later section.

The double torsion rig was mounted on a compression load cell in an Instron tensile testing machine, the load being applied at a constant crosshead displacement rate. Various speeds were employed from 0.005 to 0.5 cm min^{-1}. The samples were marked on the top surface at 2 mm intervals along the length of the guiding groove so that if continuous propagation did occur the progress of the crack could be marked on the load–displacement graph, which would later enable both a compliance calibration to be done and the crack speed to be determined. This method has obvious limitations for fast moving cracks. In this case the crack speed was measured by an electronic method. The circuit employed is shown in Fig. 2. The switches shown represent conducting tracks printed on the specimen perpendicular to the centre groove and running across it, so that as the crack propagates and each one is broken a series of steps are seen in the voltage output. By feeding this output into a transient recorder it was possible to measure crack speeds up to 400 m sec^{-1}.

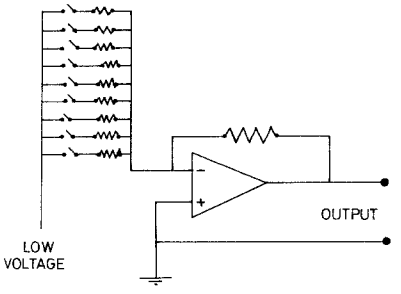

Figure 2 Crack speed measurement by conducting grids.

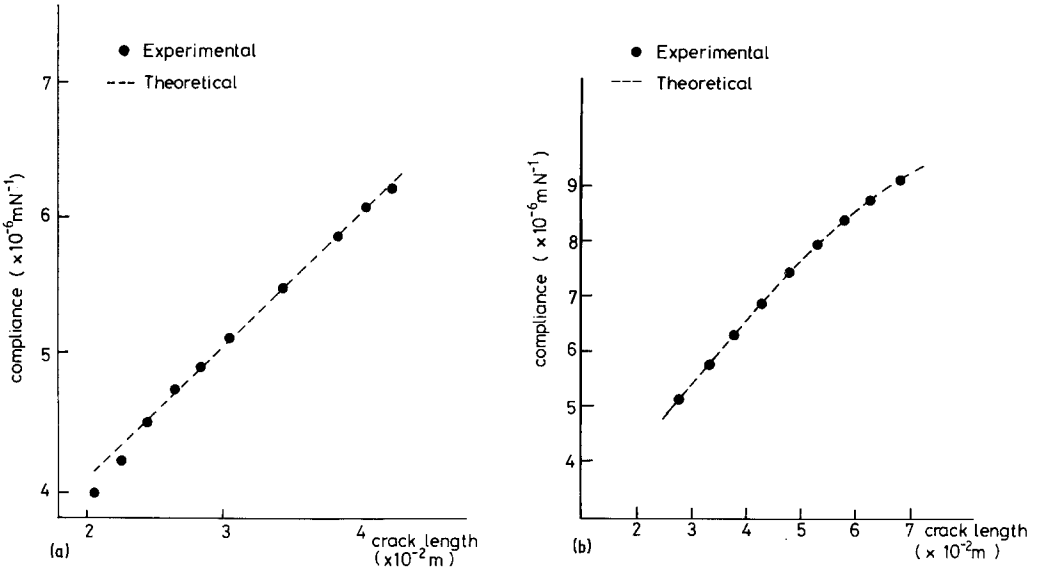

Figure 3 Comparison of the experimental and theoretical compliances for a moment arm of (a) 25 mm and (b) 7.5 mm.

As already mentioned, the stress intensity factor for crack propagation is independent of the crack length. It is given by

$$K_c^2 = \frac{P_c^2 L^2}{k_1 W t_n t^3 (1-\nu)}, \quad (1)$$

where P_c is the fracture load of propagating crack, L the moment arm, W the plate width, t the plate thickness, t_n the thickness in the plane of the crack, and ν Poisson's ratio, assumed to be constant at a value of 0.39 [19].

Following Timoshenko and Goodier [20] a correction has to be applied for plates with values of $W/2t < 10$ in order to model correctly their elastic compliance. In Equation 1 k_1 is the correction factor and is a function of $W/2t$. Values for this factor have previously been tabulated by Young and Beaumont [10].

Initial tests showed that for constant crack growth the load rose slowly as the crack propagated across the sample, whereas Equation 1 indicates that the load should remain constant. This increase is due to the decrease in the moment arm as the crosshead descended, and depends on the size of the supporting rollers, the size of the loading balls, the W/t ratio and the length of the moment arm. In most cases, it is possible to have a large enough sample width such that this effect is negligible. However, our sample width was limited by the size of plaques available. A theory has therefore been developed to model this effect which can be found in the Appendix. The result is that Equation 1 has to be modified such that

$$K_c^2 = \frac{P_c^2 \delta}{k_1 t_n t^3 W (1-\nu)} \times \left[\frac{L-(R+r+t)(\sin\theta + \theta\cos\theta)}{\theta}\right], \quad (2)$$

where δ is the crosshead displacement, θ the angle of a twisted arm to the horizontal, and R, r the radius of supporting roller and loading ball, respectively. It can be seen that for either a large moment arm L, small radii R, r or small θ (where $\delta \sim L\theta$) this equation reduces to the normal representation given by Equation 1.

Typical values for the small double torsion rig at initial crack propagation show that the moment arm has decreased by 20% from its original value. Consequently, this effect is too large to be ignored and Equation 2 has been used for all calculations of K_c.

3. Results

3.1. Validation of the test method

Initial studies were first carried out to establish the validity of Equation 2. This was readily checked by comparing the experimental compliance, given by the measured displacement divided by the measured load, with the theoretical compliance, given by Equation A4 taken from the Appendix. This was done for the two sizes of moment arm. Figs. 3a and b show the comparison of the compliances for the two rigs and it can be

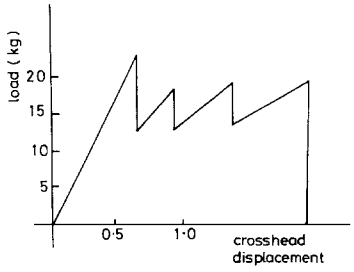

Figure 4 Stick–slip failure for material I.

seen that the correction term is much larger for the smaller moment arm, and hence the deviation of the compliance from a linear relation with crack length, a, also larger, but that it is accurately predicted by the theoretical equation derived.

3.2. Stick–slip fracture of recently moulded material (material I)

Tests were carried out on samples of newly moulded material which had been notched by pushing a razor blade into the end of the initial saw cut. The fracture behaviour shown in Fig. 4 is known as stick–slip fracture, and has been seen many times before by previous workers [2, 21, 22]. At the start of the test the load rises continually until crack initation when the crack travels unstably for a short distance. This corresponds to a rapid fall in load, the values at the points of instability and arrest giving critical values of K_c denoted by K_I and K_A, respectively. The variation with crosshead speed, $\dot{\delta}$, of K_I and K_A in continuous loading is shown in Fig. 5, calculated from a knowledge of the geometry and the values of δ and θ at each initiation and arrest. The error bars reflect the scatter in the values at each crosshead displacement rate as well as the experimental uncertainties involved. Consequently, each point represents a series of results for each particular crosshead speed. It can be seen that the values of K_I and K_A are approaching each other as the crosshead speed increases, converging to perhaps a single value for continuous crack growth at even higher speeds. A major question was whether the stick–slip fracture was a product of the notching technique, up to this point achieved by pushing a razor blade into the sample, or whether it was an inherent property of the material.

It was found that the large first peak could be removed by careful notching (i.e sawing the razor blade carefully into the sample) which reduced the possibility of a region of plastic deformation occurring in front of the starter crack. On loading, any such region tends to inhibit initial propagation of the crack and so excess stored energy builds up until fracture initiation occurs. This results in fast fracture in preference to slow propagation. A second method of notching, which also removed the chance of such a region being produced, was to drive a razor blade into the sample so that a small crack was propagated into the sample. A similar technique has been used successfully before to notch compact tension specimens [1]. The removal of this region tended to ensure that the sample failed in a stable form. However, even if the crack initially propagated in a stable manner it often became unstable at some later stage (Fig. 6). Possible reasons for this behaviour will be discussed later.

3.3. Fracture behaviour of aged material (material II)

Tests were also carried out on samples machined from plaques of the aged material. The type of failure, for samples again notched by pushing in a razor blade, was also stick–slip. It was noticeable, however, that K_I was lower than for the freshly moulded material (I). Table I shows a comparison

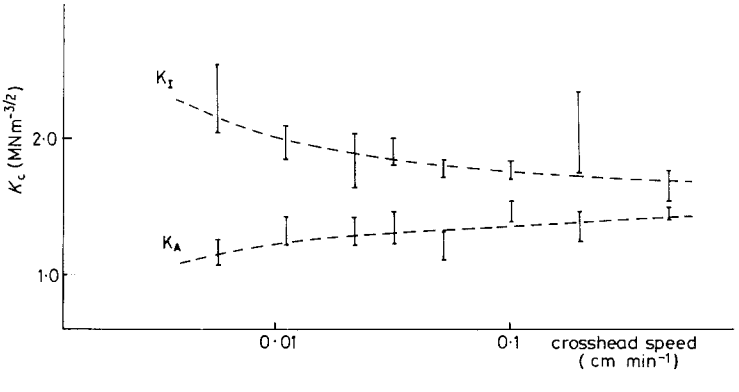

Figure 5 K_I and K_A plotted against crosshead displacement for material I.

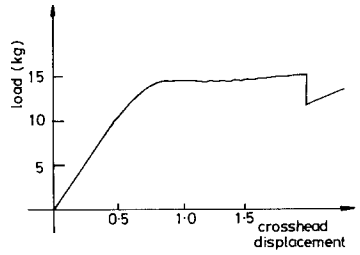

Figure 6 Stable crack propagation for material I.

of the mechanical properties of the two materials, with the aged material (II) having a higher yield stress and tensile modulus. These are reasonable trends for a material which has aged naturally for 5 years. The difference in the yield stresses shows that the freshly moulded material is more ductile and so on notching tends to form a large deformation zone. This accounts for the larger value of K_I seen in this material.

The variation of K_I and K_A with crosshead displacement rate is shown in Fig. 7. The trend is similar to that seen for the freshly moulded material (I), with the loci of the values of K_I and K_A approaching each other as the crosshead speed is increased.

Continuous crack propagation could be obtained in the aged material by introducing a starter crack free of the constraints which might have been produced by the notching technique. In the aged material it was also found possible to fatigue a precrack into the sample by cyclic loading on the Instron tensile testing machine. This method was tried with the freshly moulded material but proved unsuccessful, probably due to the material deforming and not transferring the stress to the crack tip. The aged material was stiffer and less ductile, and consequently proved much easier to fatigue. The cycling range was chosen below the load

TABLE I

	Yield stress ($MN\,m^{-2}$) ($\dot{\epsilon} = 10^{-2}\,sec^{-1}$)	Modulus (GPa)
New material	89	2.53
Old material	95	2.86

required to propagate a crack continuously (Fig. 8), as at higher loads the amount of stored energy in the sample was enough to propagate the crack a considerable distance across the sample before it could be stopped. At the lower load level it was possible to control the precrack length. Typically, samples were fatigued for 700 cycles at 1 Hz between loads of 12 and 17 kg. On subsequent loading of the fatigued sample the crack propagated continuously across the sample at a constant crack speed. It is also noticeable that the load increased slowly as the crack propagated (as predicted by the moment arm correction factor (Equation 2). A typical result obtained for a crosshead displacement rate of $0.01\,cm\,min^{-1}$ was K_c equal to $1.39\,MN\,m^{-3/2}$ for a crack speed of $9.1 \times 10^{-5}\,m\,sec^{-1}$. The fracture was not always so idealized, with stick–slip failure sometimes occurring after a period of continuous propagation, a similar effect to that noted in the freshly moulded material.

3.4. Continuous crack growth measurements

A more detailed study of continuous crack growth was carried out with the freshly moulded material (I) and the results are summarized in Fig. 9. As the results were obtained from the two double torsion rigs and for various thicknesses of material the agreement is very good showing an almost constant value of K_c of $1.4\,MN\,m^{-3/2}$ over the range of crack speeds covered. This compares with values for K_c of $1.18\,MN\,m^{-3/2}$ for slow craze growth [1]

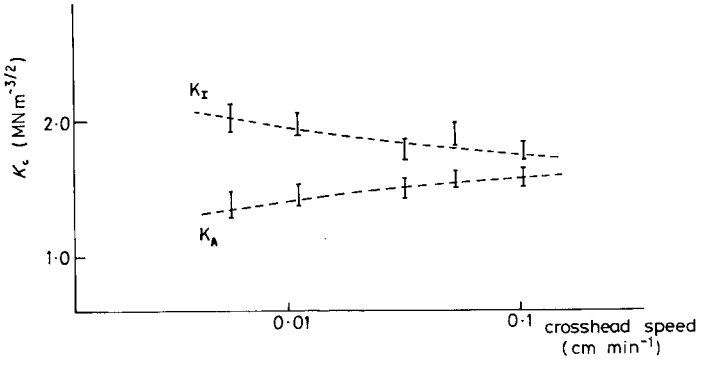

Figure 7 The variation of K_I and K_A plotted against crosshead displacement for material II.

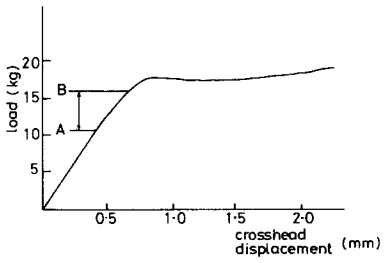

Figure 8 Stable crack propagation for material II subsequent to load cycling in the range AB.

and 2.32 MN m$^{-3/2}$ for unstable crack propagation in impact testing [23]. It appears that although for the range of crack speeds seen in these tests the value of K_c is relatively constant, there is an overall rise with increasing crack speed.

3.5. Detailed consideration of factors influencing stability of crack propagation

So far it has been shown that the method of notching affects the fracture behaviour. However, it has also been noted that there are other factors which influence the stability of crack propagation, and these will now be discussed.

The first of these is the presence, or otherwise, of a craze at the crack tip. As had previously been shown [1] a crack propagates in polyethersulphone through a craze. The formation of this craze and how it behaves on loading is, therefore, of importance with regard to the fracture behaviour. Examination of cracks in double torsion specimens in reflected light showed that there was a craze along the whole of the crack front. Fig. 10 shows the existence of this craze as a set of interference fringes caused by the craze acting as a thin wedge. By plotting the positions of the interference maxima it is then possible to ascertain the shape of the craze. In previous studies, where compact tension specimens were used, the experimental shape was compared with that predicted by the Dugdale zone model [1, 13–16]. This model describes the shape of the craze at the crack tip, on the basis that this grows to remove the stress singularity which would otherwise exist. Assuming that the craze shape is in good agreement with the Dugdale model its dimensions can then be related directly to the fracture toughness, G_c, the craze stress, σ_0, and the crack opening displacement, δ_c.

There was, however, one difficulty in obtaining a quantitative analysis of the double torsion craze shapes. To determine the critical crack opening displacement the shape of the craze, just before crack propagation occurs, is needed. For crack tips formed from compact tension specimens this is relatively easy as the portion containing the craze can be loaded in tension while being viewed in the microscope. However, it is not possible to reproduce double torsion loading and still be able to view the craze under the microscope. The results were therefore calcualted using a value for the stress intensity factor, K_c, obtained from the constant crack growth experiments, and the dimensions of the unloaded craze.

The shape of the craze fitted the Dugdale plastic zone model very well and so the Dugdale equations were then used to calculate the various fracture parameters. The results obtained are compared with previous results in Table II. It is seen that the agreement is very good, confirming that although the two tests relate to different geometries and loading conditions, the crazes produced in both tests are similar, indicative of the fracture properties of PES, and not a function of the type of test. It can be concluded that it is the craze shape over the whole crack front that is important and the shape seen at the crack tip is not very critical for this comparison.

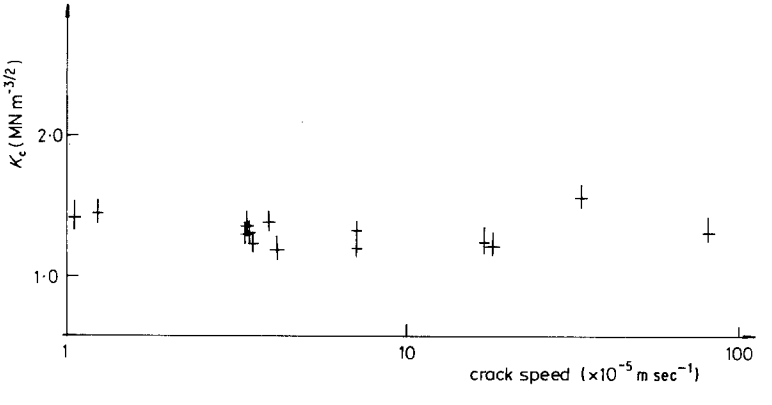

Figure 9 K_c plotted against crack speed for material II.

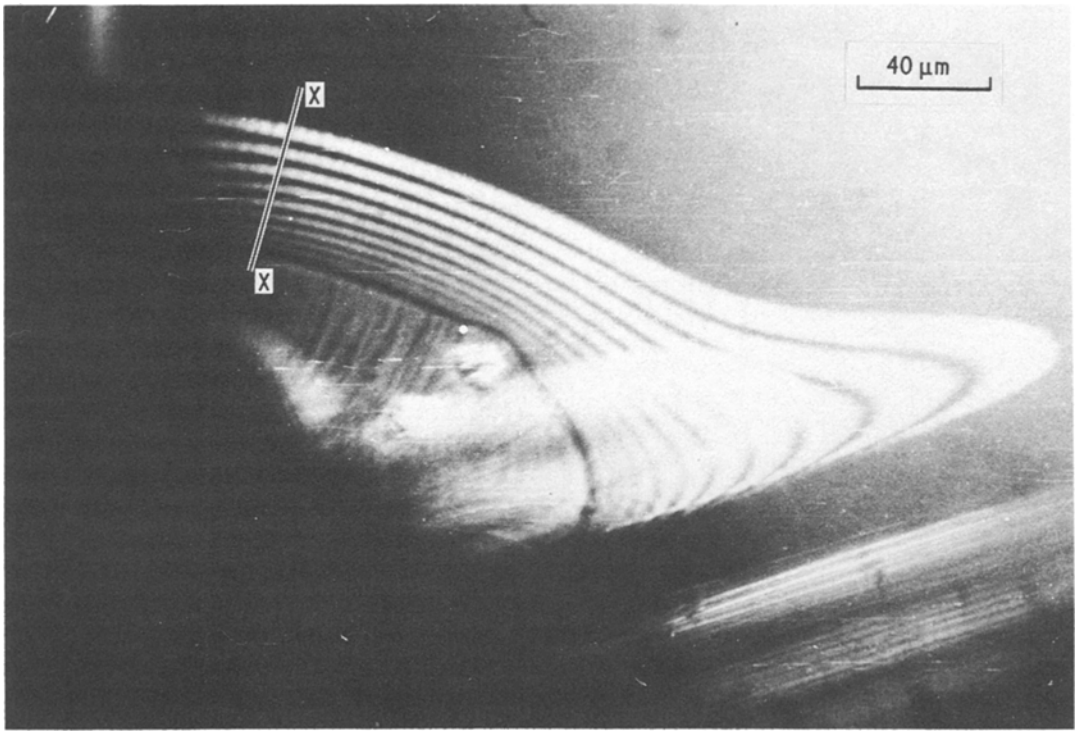

Figure 10 Interference photograph showing a craze present at the crack tip in a double torsion sample. The crack is propagating from left to right.

It proved very difficult to produce a craze in the older material II, suggesting that the balance between crazing and yielding is affected by the ageing process. Hence the reluctance of the material II to propagate in a continuous manner unless a notch was fatigued in, and in contrast the readiness of material I to propagate even with a notch produced by a razor blade is related to the formation of the craze.

So the state of the initial notch, in terms of the appearance, or otherwise, of a craze and the constraints put on it, affects whether stick–slip or continuous propagation occurs initially. The subsequent behaviour depends on other factors such as the stability of cracking, the alignment of the specimen and possible crack blunting mechanisms. There is, however, one other possibility which is linked to the craze. Consider Fig. 11 which shows the various stages of double torsion crack growth. In stage I there is the initial notch, perhaps with a craze but also possibly constrained by plastic deformation due to notching, and so on loading unstable propagation may occur. In the second state the crack tends to propagate over the whole crack front (the evidence for this is the craze present over the whole crack face) but if the crack is not long enough to provide a sufficient

TABLE II

	Compact tension	Double torsion
Craze length R (μm)	43.5 ± 2	43 ± 2
Craze stress σ_0 (MN m^{-2})	112 ± 14	134 ± 13
Crack opening displacement δ_c (μm)	4.2 ± 0.1	4.9 ± 0.9
Fracture toughness G_c (kJ m^{-2})	0.47 ± 0.025	0.66 ± 0.05

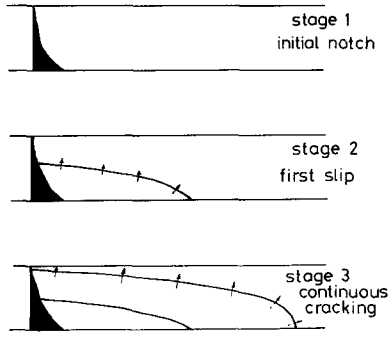

Figure 11 The stages of double torsion crack growth.

strain energy release rate then energy builds up until unstable fracture occurs. In the third and final stage a stable crack shape has been reached and a balance is achieved between stored energy and crack propagation.

These two conditions, namely an unconstrained craze along the whole crack front and the stable crack shape shown as stage 3 in Fig. 11, are therefore necessary for continuous propagation to take place.

Finally, there are other factors which control the mode of fracture. The first and most obvious is the alignment of the sample with respect to the rollers. If this is not parallel the crack tends during initial propagation to leave the guiding groove, travelling into the bulk specimen, and then arrests. On continued deformation the load to reinitiate crack growth is greater than that normally required for stable propagation and so unstable growth occurs as the crack returns to the central groove. In all cases it was found that any crack which veered off the centre groove produced unstable growth on loading again.

The second factor is the presence of some crack blunting mechanism which inhibits the initial propagation of the craze; on initiation the energy stored is greater than that required for stable growth and so unstable propagation occurs. There has been a wealth of literature discussing these crack blunting mechanisms. Young and Beaumont [3] have suggested that when a crack is loaded slowly some localized plastic deformation occurs at the crack tip and so causes blunting. This plastic deformation was thought to come from either craze branching [24] or shear yielding [25]. Similar ideas have also been postulated by Phillips *et al.* [7] and Gledhill *et al.* [2]. However, most of these experiments were conducted on epoxy-based systems where there was no evidence for the presence of a craze at the crack tip and so all the fracture properties were controlled by the behaviour of the crack tip in the absence of a craze. This is obviously a different situation to that in PES, where the craze is controlling the mode of fracture.

An alternative explanation considered by Williams and co-workers [11, 26] is the onset of thermal softening in the crack tip region. This is caused by a significant temperature rise due to a change from an isothermal process at low crack speeds to adiabatic at high crack speeds. The crack speeds encountered by Williams were of the order of 0.1 to 1 m sec^{-1} for a crack instability, so in order to assess the model it was necessary to attempt to estimate the crack speeds at instability.

The crack speed was measured, as previously explained, by a series of conducting grids across the sample. With this method it was possible to measure the crack speed and also to correlate it to the length of slip and the initiation load (Table III). The crack speeds encountered were found to be two orders of magnitude greater than those seen by Williams. It was noticeable that the crack speed was constant over the measuring range which means that any acceleration or deceleration of the crack occurred in the spacing between each grid (which was 5 mm). This agrees with work by Takahashi [27] who, by using an ultrasonic method, found that the acceleration took place in a distance from the crack tip of around 0.5 mm and that at arrest the crack stopped instantaneously.

As can be seen from Table III the crack speed is proportional to the slip distance and also to the initiation load (and hence the amount of stored energy available on initiation). This also means that the slip distance is proportional to the amount of energy available at initiation. This could explain why the values of K_I and K_A approach each other as the crosshead speed increases. As the testing rate increases the effective yield stress increases due to viscoelastic effects. This causes the size of the deformation zone around the crack tip to be smaller and hence the value of K_I to be smaller. This in turn means that the slip distance decreases and so the difference between K_I and K_A will also decrease.

It is possible to advance two explanations for crack tip blunting at successive stages of fracture, both of which are based on thermal blunting due to adiabatic heating at the crack tip. One possibility is that the heating and crack blunting occurs as the crack is being loaded. The other possibility is that the heating and crack blunting occurs when the crack is travelling very fast. So far it has been

TABLE III The variation of the crack speed with the length of the first slip

Length of slip (cm)	Crack speed (m sec^{-1})	Initiation load
2.3	168	↑
4.9	213	increasing
5	272	
10	400	↓

impossible to ascertain which, if any, of these two mechanisms could cause crack tip blunting to occur. It may be more likely that it is the presence of a craze at the crack tip, and its initiation and propagation properties, which controls the mode of fracture.

The third factor which may control the fracture is the stabiity of cracking. Gurney and Mai [28] have derived the conditions for stable crack propagation starting from the basic equation of energy balance for the creation of two surfaces. The difference in work done on the system by external forces, dW, and the increase in the stored elastic energy, dU, is equal to the energy available for the formation of crack surfaces, i.e.

$$G dA = dW - dU.$$

For a stiff testing machine it can be shown that the condition for stability is given by

$$\frac{1}{R}\left(\frac{dR}{dA}\right) \geqslant \left(\frac{d^2C}{dA^2}\Big/\frac{dC}{dA}\right) - \frac{d}{C}\left(\frac{dC}{da}\right)$$

where C is the compliance, R the specific work of fracture, and A the crack surface area. For the double torsion test it can be shown that this is equivalent to

$$\frac{1}{R}\frac{dR}{dA} > -2a\left(1+\frac{C_0}{ax}\right)^{-1}$$

if the compliance is given by $c = xa + C_0$. For a constant G_c, therefore, this means that

$$-2\left[1+\frac{C_0}{ax}\right]^{-1} < 0.$$

This will always be true but becomes less stable for larger crack lengths. This could explain an earlier observation that the mode of fracture sometimes becomes stick–slip after a long portion of continuous growth (Fig. 6).

4. Conclusions

Two distinct modes of fracture have been found for PES tested in double torsion. One is unstable and is characterized by crack growth in a series of jumps, the other stable characterized by continuous crack growth at constant speed. By determining the factors which controlled the mode of fracture and taking into account changes in moment arm of the rig it was possible to produce continuous crack growth over a range of crack speeds and a relatively constant value of $K_c = 1.4\,\mathrm{MN\,m^{-3/2}}$. This value of K_c, together with measurements of the length of the craze which is observed at the crack tip for continuous crack growth gave a value for crack opening displacement and craze stress which agrees well with values previously determined from compact tension tests. In addition to the presence of a craze there were other factors controlling the fracture mode, notably the shape and size of the crack, the alignment of the sample, crack blunting effects and the stability of the double torsion configuration.

Appendix

Consider the specimen after the crosshead has moved through a distance δ as shown in Fig. A1. The effective moment has decreased from $PL/2$ to

$$M = \frac{P}{2}L'' \cos\theta \qquad \text{(A1)}$$

where L'' and $\cos\theta$ are indicated in the figure. Since

$$L'' = \frac{L'}{\cos\theta} - t\tan\theta \qquad \text{(A2)}$$

and

$$L' = L[1-(R+r)\sin\theta] \qquad \text{(A3)}$$

it follows that

$$M = \frac{P}{2}[L-(R+r+t)\sin\theta]. \qquad \text{(A4)}$$

From elastic analysis

$$M = (k_1/2)Wt^3G(\theta/a) \qquad \text{(A5)}$$

and so it follows that

$$P = \frac{k_1Wt^3E\theta/a}{2[L-(R+r+t)\sin\theta](1+\nu)}. \qquad \text{(A6)}$$

By definition the specimen compliance $C = \delta/P$ and so

$$C = \frac{2\delta a[L-(R+r+t)\sin\theta](1+\nu)}{k_1Wt^3E\theta}. \qquad \text{(A7)}$$

This can be rewritten as

$$C = \frac{\delta a[L-x\sin\theta]}{A\theta}, \qquad \text{(A8)}$$

where $x = R + r + t$ and $A = k_1Wt^3E/2(1+\nu)$.

Because δ and θ are functions of a we have

$$\frac{dC}{da} = \left(\frac{\partial C}{\partial a}\right)_{\theta,\delta} + \left(\frac{\partial C}{\partial\theta}\right)_{\delta}\frac{d\theta}{da} + \left(\frac{\partial C}{\partial\delta}\right)_{\theta}\cdot\frac{d\delta}{da}. \qquad \text{(A9)}$$

Experiment shows that to a good approximation

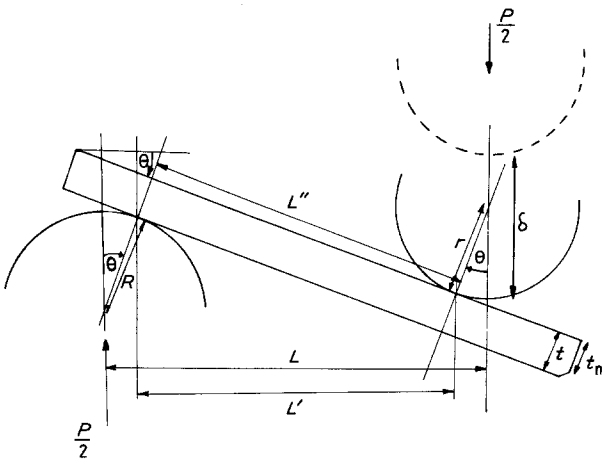

Figure A1 Double torsion test geometry.

$$\theta \doteqdot C_1(a - a_i)$$
$$\text{and} \qquad \delta \doteqdot K_1(a - a_i) \qquad \text{(A10)}$$

where a_i is the initial crack length.

Differentiation of Equation A8 to Equation A9, using the experimental results (Equation A10) shows that

$$\frac{dC}{da} \doteqdot \left[\frac{L - x\sin\theta}{A\theta}\right]\delta - \frac{\delta x\cos\theta}{A}, \qquad \text{(A11)}$$

for the usual situation where $a \gg a_i$.

Using the Irwin–Kies relation

$$K_c^2 = \frac{P^2}{2t}\frac{E}{1-\nu^2}\frac{dC}{da}, \qquad \text{(A12)}$$

it follows that

$$K_c = \frac{P^2\delta}{t_n k_1 W t^3(1-\nu)} \times \left[\frac{L-(R+r+t)(\sin\theta+\theta\cos\theta)}{\theta}\right]. \qquad \text{(A13)}$$

N.B. This equation reduces to Equation 1 in the limit of small θ.

References

1. P. J. HINE, R. A. DUCKETT and I. M. WARD, *Polymer* **22** (1981) 1745.
2. R. A. GLEDHILL, A. J. KINLOCH, S. YAMINI and R. J. YOUNG, *Polymer* **19** (1978) 574.
3. R. J. YOUNG and P. W. R. BEAUMONT, *J. Mater. Sci.* **11** (1976) 776.
4. D. C. PHILLIPS and J. M. SCOTT, *ibid.* **9** (1974) 1202.
5. B. W. CHERRY and K. W. THOMPSON, *Int. J. Fract.* **14** (1978) R17.
6. S. YAMINI and R. J. YOUNG, *Polymer* **18** (1977) 1075.
7. D. C. PHILLIPS, J. M. SCOTT and M. JONES, *J. Mater. Sci.* **13** (1978) 311.
8. R. J. YOUNG and P. W. R. BEAUMONT, *ibid.* **10** (1975) 1343.
9. D. KUNZ and P. W. R. BEAUMONT, *ibid.* **16** (1981) 3141.
10. R. J. YOUNG and P. W. R. BEAUMONT, *ibid.* **12** (1977) 684.
11. G. P. MARSCHALL, L. H. COUTS and J. M. WILLIAMS, *ibid.* **9** (1974) 1409.
12. P. W. R. BEAUMONT and R. J. YOUNG, *ibid.* **10** (1975) 1334.
13. H. R. BROWN and I. M. WARD, *Polymer* **14** (1973) 469.
14. W. DÖLL and G. W. WEIDMAN, *Colloid. Polym. Sci.* **254** (1976) 205.
15. S. A. VAVAKIN, Yu. I. KOZYREV and R. Z. SALGANIK, *Izvest. Akad. Nauk SSR Mekh Tverd Tela* **11** (1976) 111.
16. D. S. DUGDALE, *J. Mech. Phys. Solids* **8** (1960) 100.
17. J. G. EVANS, *J. Mater. Sci.* **7** (1972) 1137.
18. J. A. KIES and A. B. J. CLARK, in "Fracture 1969", edited by P. L. Pratt (Chapman and Hall, London, 1969) p. 483.
19. K. V. GOTHAM and S. TURNER, *Polymer* **15** (1974) 665.
20. S. TIMOSHENKO and J. N. GOODIER, "Theory of Elasticitiy", 2nd Edn. (McGraw-Hill, New York, 1951).
21. R. A. GLEDHILL and A. J. KINLOCH, *Polymer* **17** (1976) 727.
22. K. SELBY and L. E. MILLER, *J. Mater. Sci.* **10** (1975) 12.
23. P. J. HINE, PhD thesis, University of Leeds (1981).
24. G. P. MARSHALL, L. E. CULVER and J. G. WILLIAMS, *Int. J. Fracture* **9** (1977) 295.
25. R. E. ROBERTSON, *J. Chem. Phys.* **44** (1966) 3950.
26. J. G. WILLIAMS and J. M. HODGKINSON, *Proc. Roy. Soc.* **375** (1981) 231.
27. K. TAKAHASHI, M. KIMURA and S. HYODO, *J. Mater. Sci.* **13** (1978) 2718.
28. C. GURNEY and Y. M. MAI, *Eng. Fract. Mech.* **4** (1972) 853.

Recieved 23 January
and accepted 31 January 1984